Analytical Methods

Cite this: *Anal. Methods*, 2012, **4**, 3779

www.rsc.org/methods

PAPER

Electroanalytical properties of cytochrome c with direct electron transfer on graphene/gold nanoparticles chitosan modified glass carbon electrode†

Fucheng Li,[a] Yan Mo,[a] Dan Xiao,[ab] Hongyan Yuan*[b] and Yong Guo*[a]

Received 16th July 2012, Accepted 7th September 2012
DOI: 10.1039/c2ay25763g

A nitrite (NO_2^-) sensor has been fabricated by immobilizing cytochrome c (Cyt c) on a graphene/gold nanoparticle-chitosan (Gra/Au NPs–Chit) modified glass carbon electrode (GCE). Graphene/gold nanoparticles (Gra/Au NPs) nanocomposite was prepared by dispersing graphene in an aqueous solution of β-cyclodextrin (β-CD) and hydrogen tetrachloroaurate and followed by $NaBH_4$ reduction. An aliquot of Gra/Au NPs in a 0.50 wt% chitosan solution was drop-coated on the surface of a GCE to form a Gra/Au NPs–Chit/GCE which was subsequently adsorbed with Cyt c. The Cyt c–Gra/Au NPs–Chit/GCE shows a quasi-reversible cyclic voltammetric redox couple at a formal potential of −0.037 V (*vs.* SCE) in 0.10 M pH 7.0 phosphate buffer solution, suggesting that Gra/Au NPs–Chit film offers a biocompatible microenvironment for the Cyt c. It was found that the Cyt c–Gra/Au NPs–Chit sensor displays good electrocatalytic activity for NO_2^- oxidation at a relatively low working potential. The sensor possesses a linear response range of 10.0–420.0 μM NO_2^- with a correlation coefficient of 0.9989 and a sensitivity of 110.0 μA mM^{-1}. The limit of detection is determined as 2.46 μM NO_2^- based on a signal-to-noise ratio of 3. The proposed sensor has been applied successfully to the determination of NO_2^- in spiked and real water samples.

1. Introduction

Carbon nanomaterials have received considerable attention in the fields of electroanalysis and electrocatalysis.[1–3] Among the carbon nanomaterials, graphene is considered as one of the most promising candidates and it has attracted much scientific and technological interest in recent years.[4,5] Since graphene has a long range π–π conjugation 2D lattice structure, it can produce extraordinary thermal, mechanical and electrical properties. Thus, the application of graphene in bioelectronics and biosensors has been widely explored.[6,7]

Direct electrochemistry of enzyme or redox protein refers to the direct electron transfer (DET) between the active center of enzyme or protein and the electrode surface without passing through any media. The active center of an enzyme is deeply embedded in the protein which makes DET very difficult to realize. Many research groups have expended much effort to study DET. Li Niu *et al.*[6] developed an excellent DET glucose biosenor using polyethylenimine-functionalized ionic liquid dispersed polyvinylpyrrolidone-protected graphene. Bin Wang and co-workers[8] immobilized horseradish peroxidase (HRP) on a silica-HAp film modified electrode for H_2O_2 biosensing based on the fast electron communication between HRP and the modified electrode. Guo *et al.* reported the electrochemical behavior of hemoglobin (Hb) on a carbonized titania nanotube modified electrode. The heterogeneous electron transfer rate constant of Hb on this electrode was 108 s^{-1}, demonstrating a rapid electron exchange between electrode and heme.[9] Cytochrome c (Cyt c) is an important heme-containing redox protein and has been widely used to study electron transfer. *In vivo*, it displays a crucial role for electron transfer between Cyt c reductase and Cyt c oxidase. Since Kuwana and Yeh[10] reported the DET of Cyt c, different approaches[11–15] have been explored to enhance DET of this protein molecule. So far Cyt c has been extensively used for detecting H_2O_2,[12,15–17] NO,[18] superoxide[13] and nitrite (NO_2^-)[11,19] owing to its excellent electrocatalysis activity. During the past decade, carbon nanomaterials have been widely employed and proven to improve electron transfer between the electrode surface and the active center of Cyt c.

Nitrite is generally used as inhibitor and an additive in meat production for antimicrobial action.[11,20] It is an active intermediate species in the nitrogen cycle. Blood pigment can readily react with NO_2^- to form metal–hemoglobin, which results in a loss of the oxygen transfer ability of blood pigment. As such, the development of a selective and sensitive method to detect NO_2^- is of particularly importance. Electrochemical measurement is recognized as a simple, easy and highly sensitive method for NO_2^- determination. For instance, manganese dioxide[21] and

[a]*Key Laboratory of Green Chemistry and Technology, Ministry of Education, College of Chemistry, Sichuan University, Chengdu 6140064, People's Republic of China. E-mail: guoy@scu.edu.cn; Fax: +86-028-85416029; Tel: +86-028-85415029*
[b]*College of Chemical Engineering, Sichuan University, Chengdu 610065, People's Republic of China. E-mail: yuan_hy@scu.edu.cn*
† Electronic supplementary information (ESI) available. See DOI: 10.1039/c2ay25763g

CS@PB/GNS-CNS[22] modified electrodes have been fabricated for the determination of NO_2^-. Jiangyi Wang and co-authors[23] employed dual-region Au NPs and Pt NPs modified electrodes for simultaneous detection of glucose and nitrite. However, most of these electrochemical sensors required the use of a relatively high working potential. In this work, we report the development of a low working potential sensor for NO_2^- determination. The proposed NO_2^- sensor was fabricated from Cyt c-immobilized graphene/gold nanoparticles chitosan (Cyt c–Gra/Au NPs–Chit) modified glass carbon electrode (GCE). Cyt c was directly immobilized on the Gra/Au NPs nanocomposites/chitosan modified GCE by a simple adsorption procedure. The DET behavior of Cyt c was studied in detail. Our proposed Cyt c–Gra/Au NPs–Chit modified GCE displays high sensitivity to NO_2^- and can function well at low applied working potentials. Finally, the developed Cyt c–Gra/Au NPs–Chit sensor was applied successfully to detect NO_2^- in spiked water and wastewater samples.

2. Experimental

2.1 Reagents and materials

Graphite powder was purchased from Shanghai Huayi Group Hua Yuan Chemical Industry Co., Ltd. (Shanghai, China). Chitosan (Acros Organics, Geel, Belgium) was dissolved in 2.0% acetic acid solution. 1.0 wt% β-cyclodextrin (Tianjin Kermel Chemical Reagents Co. Ltd., Tianjin, China) was prepared by dissolving β-cyclodextrin (β-CD) in redistilled water. Hydrogen tetrachloroaurate (III) ($HAuCl_4$) was obtained from Aldrich (Milwaukee, WI, USA). Sodium borohydride ($NaBH_4$) was purchased from Alfa Aesar (Taylor, MI, USA). Horse heart cytochrome c was obtained from Sigma (St. Louis, MO, USA) and used without further purification. All other reagents were of analytical grade and used as received. All aqueous solutions were prepared using redistilled water. Phosphate buffer solution (PBS, 0.10 M, pH 7.0) was prepared by mixing a stock standard solution of Na_2HPO_4 and NaH_2PO_4 and adjusting the pH with 0.10 M NaOH or H_3PO_4.

2.2 Apparatus

All electrochemical measurements including cyclic voltammetry (CV) and electrochemical impedance spectroscopy (EIS) were performed on an Autolab PGSTA 30 electrochemical work station (ECO Chemie BV, Utrecht, Netherlands) and controlled by GPES and Fra software. A conventional three-electrode system comprising a bare GCE or a Cyt c–Gra/Au NPs–Chit modified GCE working electrode, a saturated calomel electrode (SCE) as reference electrode and a platinum wire as the auxiliary electrode was employed for electrochemical measurements. The GCE (3 mm diameter) was polished to a mirror-like surface with 1.0, 0.3 and 0.05 μm alumina powder successively and rinsed with redistilled water. The polished GCE was sonicated in redistilled water, nitric acid and ethanol, respectively, and subjected to twenty CV scans at scan potential of −0.20 V to 0.80 V in 0.50 M H_2SO_4. Prior to all electrochemical experiments, the solutions were deoxygenated by a stream of high purity nitrogen (N_2) for 15 min. N_2 atmosphere was maintained over the measurement and all experiments were performed at room temperature.

The morphology of Gra/Au NPs nanocomposite was examined by a FEI INSPECT F50 field emission scanning electron microscope (Hillsboro, OR, USA). X-ray photoelectron spectroscopic (XPS) analysis was performed on a Kratos XASM 800 X-ray photoelectron spectrometer (Manchester, UK).

2.3 Preparation of Gra/Au NPs–Chit modified glass carbon electrode

Graphene was prepared by chemical reduction of graphite oxide. Briefly, graphite oxide was synthesized by a modified Hummers' method.[24,25] First, about 100 mg graphite oxide was dispersed in 100 mL redistilled water by ultra-sonication for 1 h. The obtained homogeneous graphite oxide dispersion solution was added to a 4.0 mL 0.50 wt% chitosan and 2.0 g $NaBH_4$ solution and reacted at 100 °C in oil bath for 4 h. Finally, the wrinkled graphene sheets obtained were dried in vacuum at 35 °C overnight.

β-CD is composed of seven glucose units and has a hydrophobic inner cavity and hydrophilic exterior. It is commonly employed to disperse carbon nanomaterials[26,27] due to this structure. About 40 mg of graphene was ultra-sonicated for 1 h in 40 mL 1.0 wt% β-CD solution and then, following the addition of 150 μL of 10 g L^{-1} $HAuCl_4$ solution, stirred for 30 min . Next 2.5 mL of 1.0 M $NaBH_4$ in 0.10 M NaOH was added into the mixture solution. The reaction mixture was stirred for 2 h, cooled to room temperature, filtered and washed with copious amounts of water to obtain the Gra/Au NPs nanocomposite. Finally, the Gra/Au NPs nanocomposite was dried in vacuum at 35 °C overnight.

The Gra/Au NPs–Chit suspension was prepared by dispersing 5.0 mg Gra/Au NPs nanocomposite in 1.0 mL of 0.50 wt% chitosan solution by sonication. 4.0 μL of Gra/Au NPs–Chit suspension was coated on the surface of a GCE and left to dry under ambient conditions. Afterwards, the Gra/Au NPs–Chit/GCE was immersed into a Cyt c solution (3 mg mL^{-1}, pH 7.0 PBS) at 4 °C for 24 h. During this process, Cyt c was successfully immobilized on Gra/Au NPs–Chit/GCE to obtain a Cyt c–Gra/Au NPs–Chit modified GCE. The Cyt c–Gra/Au NPs–Chit/GCE was stored in PBS at 4 °C when not in use.

3. Results and discussion

3.1 SEM and XPS of Gra/Au NPs nanocomposite

Fig. 1(a) shows the SEM image of Gra/Au NPs and reveals that Au NPs were successfully deposited on the graphene sheet. The spherical Au NPs obtained, with an average diameter of *ca.* 37 nm, were homogeneously distributed on the surface of graphene. Fig. 1(b) displays the XPS spectrum of the Gra/Au NPs nanocomposite. Au $4f_{5/2}$ and Au $4f_{7/2}$ peaks appeared at *ca.* 87.4 and 83.9 eV which is consistent with the literature values.[28] These results supported the observation that Au NPs decorated on graphene were obtained.

3.2 Electrochemical characteristics of Gra/Au NPs–Chit/GCE

Electrochemical impedance spectroscopy (EIS) was employed to study the features of the surface electron transfer properties. Fig. 2(a) depicts typical Nyquist plots (Z_{im} *vs.* Z_{re}) of different

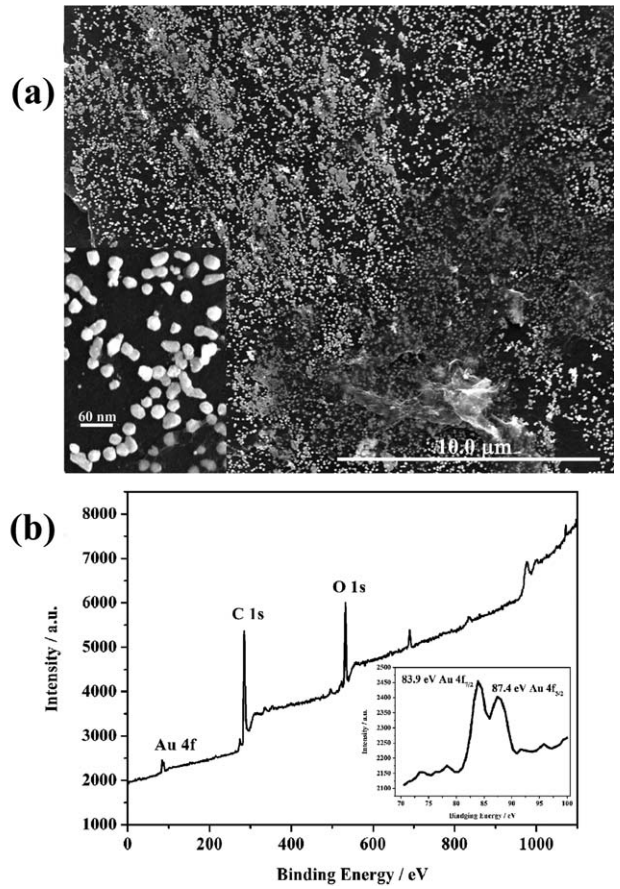

Fig. 1 (a) SEM image of the Gra/Au NPs. Inset displays the SEM image of Au NPs. (b) XPS spectrum of Gra/Au NPs nanocomposite. Inset shows the Au 4f doublet.

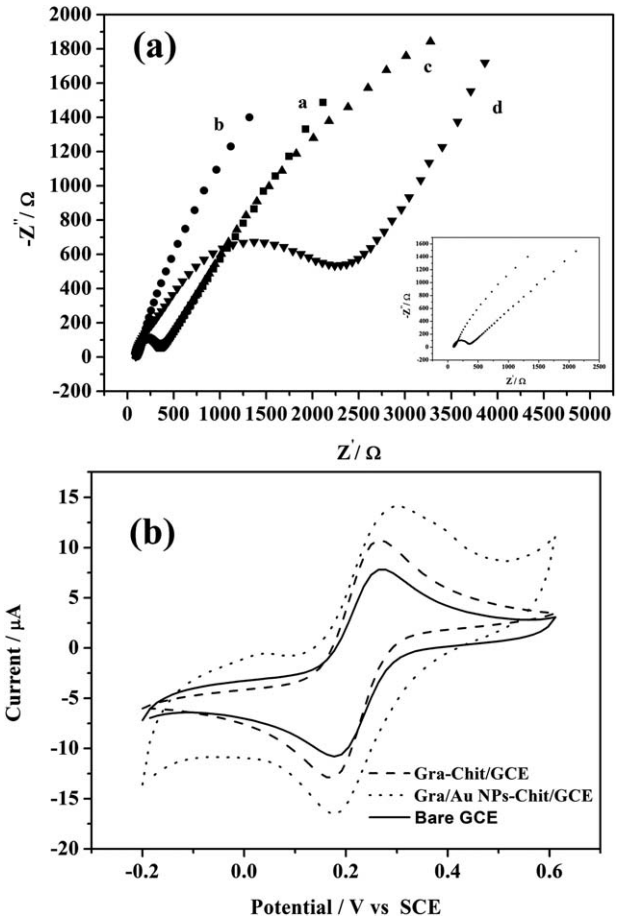

Fig. 2 (a) Nyquist plots of different electrodes in 5.0 mM $Fe(CN)_6^{3-/4-}$ with 0.10 M KCl as the supporting electrolyte: (a) bare GCE, (b) Gra/Au NPs–Chit/GCE, (c) Chit/GCE, and (d) Cyt c–Gra/Au NPs–Chit/GCE. The frequency range is 0.01 Hz to 100 kHz. The amplitude is 0.010 V. The inset depicts the Nyquist plots of bare GCE and Gra/Au NPs–Chit/GCE. (b) Cyclic voltammograms of bare GCE (solid line), Gra–Chit/GCE (dashed line), Gra/Au NPs–Chit/GCE (dotted line) in 1.0 mM $K_3[Fe(CN)_6]$ and 1.0 M KCl at 50 mV s^{-1}.

electrodes: (a) bare GCE, (b) Gra/Au NPs–Chit/GCE, (c) Chit/GCE, and (d) Cyt c–Gra/Au NPs–Chit/GCE in 5.0 mM $[Fe(CN)_6]^{3-/4-}$ solution. All Nyquist plots contain a semicircle in the high frequency range and are linear at low frequencies. The semicircle diameter represents the electron transfer resistance (R_{et}) of the electrode. The linear part is derived from the finite-length Warbury diffusion impedance. R_{et} of Chit/GCE (289.4 Ω) is larger than that of the bare GCE (271.5 Ω), suggesting that a layer of chitosan is formed at the bare GCE surface, which hinders electron transfer from the elcctrode. R_{et} of Gra/Au NPs–Chit/GCE (102.7 Ω) is much lower than that of bare GCE, demonstrating that the Gra/Au NPs on the electrode surface speed up the electron transfer process of the Fe^{2+}/Fe^{3+} redox couple. When Cyt c is adsorbed on the Gra/Au NPs film, the R_{et} increases to 2.011 kΩ, which indicates that Cyt c is successfully immobilized on the Gra/Au NPs–Chit/GCE surface.

Fig. 2(b) displays the CV responses of Gra/Au NPs–Chit/GCE, Gra–Chit/GCE and bare GCE in 1.0 mM $K_3[Fe(CN)_6]$ solution with 1.0 M KCl as the supporting electrolyte. A pair of electrochemical redox peaks was obtained, which indicates that reversible electron-transfer reactions take place on the electrode surfaces. The cathodic and anodic currents at the Gra–Chit/GCE are higher than those of the bare GCE. This demonstrates that the electrochemical active area of GCE is increased by the Gra decorated surface. Enhanced current response on Gra/Au NPs–Chit/GCE may be due to highly conducting Au NPs on the Gra. The Au NPs may act as an electron-transfer channel, which further improves the conductivity of the Gra film.[29]

3.3 Direct electron transfer of cytochrome c immobilized on the Gra/Au NPs–Chit/GCE

CVs were performed to investigate the electrochemical characteristics of Cyt c–Gra/Au NPs–Chit/GCE in N_2-saturated PBS. Fig. 3(a) shows the CVs of bare GCE, Cyt c–Chit/GCE, Gra/Au NPs–Chit/GCE and Cyt c–Gra/Au NPs–Chit/GCE. A pair of quasi-reversible redox peaks (curve d) were obtained at the Cyt c–Gra/Au NPs–Chit/GCE. By contrast, no obvious peaks were found at the other electrodes (Fig. 3 curves a–c). The formal potential of Cyt c–Gra/Au NPs–Chit/GCE is −0.037 V (*vs.* SCE), which is more negatively shifted as compared with Cyt c (0.017 V) in PBS. The negative shift of potential reveals an interaction between Gra/Au NPs and heme.[30] This result proves that DET could be achieved between the protein molecule and the electrode surface. In addition, the background current of

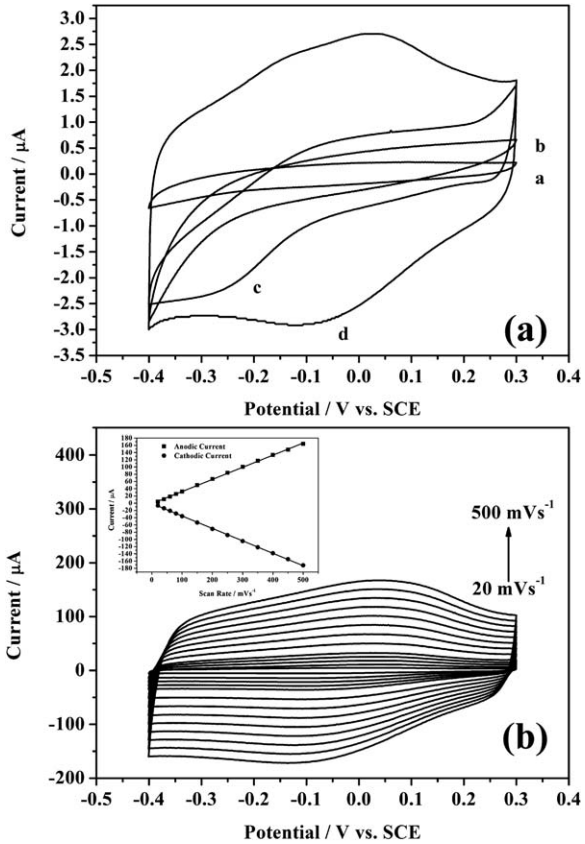

Fig. 3 (a) Cyclic voltammograms of various electrodes (a) bare GCE, (b) Cyt c–Chit/GCE, (c) Gra/Au NPs–Chit/GCE, and (d) Cyt c–Gra/Au NPs–Chit/GCE in N_2-saturated PBS. Scan rate 50 mV s^{-1}. (b) CVs of Cyt c–Gra/Au NPs–Chit/GCE in 0.10 M pH 7.0 PBS at various scan rates: 20, 40, 60, 80, 100, 150, 200, 250, 300, 350, 400, 450 and 500 mV s^{-1}. Inset displays the plot of peak current (I_p) *versus* scan rate.

Gra/Au NPs–Chit/GCE is higher than that of bare GCE, owing to the larger electrode surface area of Gra/Au NPs–Chit/GCE.

The effect of scan rate on the voltammetric behavior of Cyt c was studied. Fig. 3(b) shows that both anodic and cathodic peak currents increase linearly with scan rates from 20 to 500 mV s^{-1}. These results indicate that the electrochemical reaction is a typical surface-control process according to the Laviron equation (1):[16,31]

$$I_p = n^2F^2v\Gamma A/4RT \quad (1)$$

where I_p is the peak current, n is the electron transfer numbers, A is the surface area of the working electrode (cm^2), Γ is the surface coverage (mol cm^{-2}), *i.e.*, the surface concentration of electroactive substance, and other parameters are the usual physical constants. The surface coverage of Cyt c was calculated to be 1.91×10^{-9} mol cm^{-2} which is larger than the literature value.[11,16,29] This is due to the good immobilization ability of Gra/Au NPs–Chit film to biomolecules. When CV scan rates increase, redox potentials (E_{pa} and E_{pc}) of Cyt c do not change much, which can be attributed to the fast electron transfer between Cyt c and electrode surface.[8] These results indicate that the Gra/Au NPs–Chit composite offers a biocompatible microenvironment to immobilize as well as stabilize Cyt c on the GCE.

3.4 Analytical performance of Cyt c–Gra/Au NPs–Chit/GCE

Fig. 4 shows CV scans of (a) bare GCE, (b) Gra/Au NPs–Chit/GCE and (c) Cyt c–Gra/Au NPs–Chit/GCE in PBS containing 200 μM NO_2^-. Curve (d) in Fig. 4 is the CV curve of Cyt c–Gra/Au NPs–Chit/GCE in PBS without NO_2^-. No distinct oxidation peak was found for the bare GCE while a small anodic peak at 0.83 V was observed for the Gra/Au NPs–Chit/GCE. A well-defined oxidation peak at 0.78 V was identified as Cyt c–Gra/Au NPs–Chit/GCE in PBS containing NO_2^- but no anodic peak was found in the absence of NO_2^-. NO_2^- therefore contributes to the oxidation peak at +0.78 V, which was subsequently chosen as the optimal working potential for NO_2^- detection. Our proposed Cyt c–Gra/Au NPs–Chit sensor shows efficient electrocatalytic behavior toward NO_2^- at a much lower working potential than other previously reported sensors.[11,21,22]

Fig. 5 shows CVs of Cyt c–Gra/Au NPs–Chit/GCE in 0.10 M deoxygenated PBS solution containing various concentrations of NO_2^-. The oxidation peak current increases with increased concentration of NO_2^-. Fig. 6 shows a typical amperometric-time response curve for the Cyt c–Gra/Au NPs–Chit/GCE with successive additions of 20 μL of 50 mM $NaNO_2$ into a stirred 50 mL PBS (0.10 M, pH 7.0) solution. The current increases progressively after each addition of NO_2^-. The inset of Fig. 6 depicts the calibration curve, current *vs.* NO_2^- concentration, for Cyt c–Gra/Au NPs–Chit/GCE. The response current displays good linear behavior in the range 10.0 μM to 420.0 μM NO_2^- with a sensitivity of 110.0 μA mM^{-1} and a correlation coefficient of 0.9989. This sensitivity is larger than that of a previous sensor.[21,22] The limit of detection is determined to be 2.46 μM based on a signal-to-noise ratio of 3. That the sensor exhibits a rapid response is observed from the current, which reached 95% of the equilibrium value about 5 s after the addition of nitrite.

3.5 Repeatability, reproducibility and stability

Good repeatability and stability are important characteristics of a sensor for practical applications. Our proposed Cyt c–Gra/Au NPs–Chit/GCE sensor shows good repeatability for NO_2^- analysis. There is 2.67% relative standard deviation (RSD) for 5

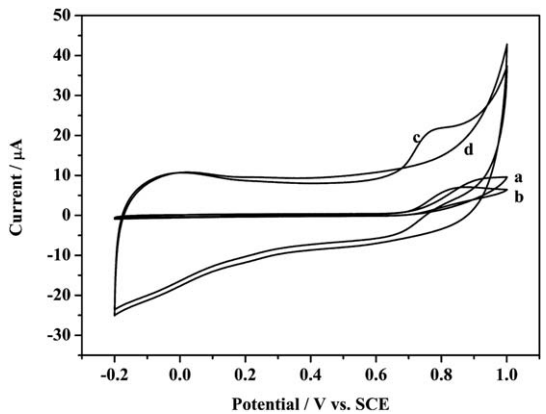

Fig. 4 Cyclic voltammograms of the (a) bare GCE, (b) Gra/Au NPs–Chit/GCE and (c) Cyt c–Gra/Au NPs–Chit/GCE in N_2-saturated 0.10 M PBS (pH 7.0) containing 200 μM nitrite at 50 mV s^{-1}, and (d) Cyt c–Gra/Au NPs–Chit/GCE in PBS without nitrite.

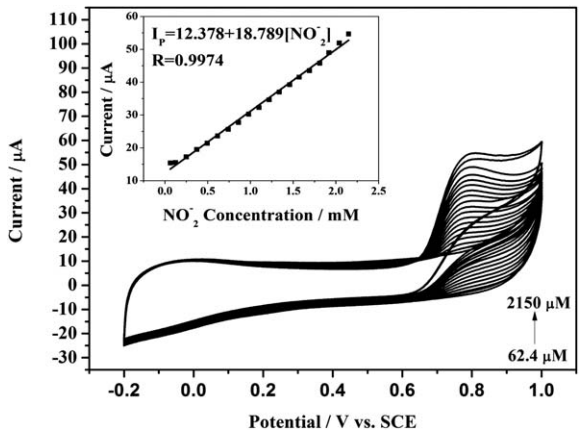

Fig. 5 Cyclic voltammograms of Cyt c–Gra/Au NPs–Chit/GCE in PBS containing different concentrations of nitrite (62.4–2150 μM) at 50 mV s^{-1}. Inset displays the calibration curve of peak current *vs.* NO_2^- concentration.

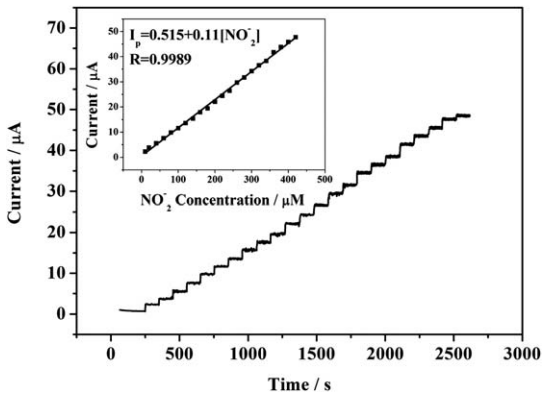

Fig. 6 Typical amperometric response of the Cyt c–Gra/Au NPs–Chit/GCE upon successive additions of 20 μL of 50 mM $NaNO_2$ into a stirred 50 mL PBS solution. The applied potential is +0.78 V. Inset depicts the calibration curve of current *vs.* NO_2^- concentration.

successive determinations of 200 μM NO_2^-. The reproducibility of fabrication of Cyt c–Gra/Au NPs–Chit/GCE was assessed by simultaneously preparing five Cyt c–Gra/Au NPs–Chit/GCEs. Each Cyt c–Gra/Au NPs–Chit/GCE was exposed to 200 μM NO_2^- and the RSD of the oxidation is 3.7%, demonstrating that the fabrication of Cyt c–Gra/Au NPs–Chit/GCE is highly reproducible. The storage stability of Cyt c–Gra/Au NPs–Chit/GCE at 4 °C was assessed by intermittently exposing it to a standard solution of 200 μM NO_2^-. The current response drops by 2.1 and 5.9% after 2-day and 2-week storage, respectively. The electrode retained 83.0% current response after a month, indicating that the proposed Cyt c–Gra/Au NPs–Chit/GCE exhibited good long-term stability.

3.6 Interference test

In real samples, some co-existing inorganic ions and electroactive species may affect the sensor response for nitrite. In this work, potential interferents in the determination of nitrite on the sensor was evaluated by successively adding each interferent (10 mM) into pH 7.0 PBS as displayed in Fig. S2 (ESI†). The nitrite sensor did not show any significant response to the ions Na^+, K^+, Ca^{2+}, NH_4^+, F^-, Cl^-, Br^-, SO_4^{2-}, NO_3^-, $H_2PO_4^-$, HPO_4^{2-}, glucose or fructose. However, the sensor did show a slight response to 10 mM L-ascorbic acid but this did not affect the detection of nitrite in real samples. The nitrite sensor maintains a good response to 200 μM nitrite in the presence of these ions and electroactive species. The results demonstrate the good selectivity of the proposed sensor.

3.7 Determination of nitrite in wastewater samples

To assess the feasibility of the Cyt c–Gra/Au NPs–Chit sensor in practical applications, the NO_2^- content was determined in spiked water and wastewater samples. Industrial wastewater was collected from a local food factory. A sample was diluted 10 times and simultaneously analyzed by our proposed sensor and the classical Griess method.[32] A recovery test was carried out by adding known quantities of NO_2^- to tap water and wastewater. Table 1 summarizes the results of the analysis and recovery. The results obtained by our proposed method are consistent with that of the Griess method. The recoveries are 94.1–103%, demonstrating the validity of our proposed sensor. In order to further evaluate the stability of the proposed sensor to detect NO_2^- in real samples, the sensor was kept in PBS at 4 °C for two weeks and then applied to determine NO_2^- in the wastewater sample. The results were satisfactory (wastewater 2[b] in Table 1). In summary, our proposed sensor offers an alternative method for the determination of NO_2^- in real samples.

Table 1 Determination of nitrite in spiked tap water and wastewater samples

Sample	Added ($\times 10^{-5}$ M)	Proposed method found ($\times 10^{-5}$ M)[a]	Recovery (%)	RSD (%)	Griess method found ($\times 10^{-5}$ M)[a]	Relative error (%)
Spiked water	9.64	9.83	102	2.56	9.72	1.12
	37.8	36.3	96.0	1.27	38.3	−1.32
Wastewater 1[b]	0.0	17.1	—	0.837	18.2	−6.43
	15.5	33.7	103	1.44	—	—
Wastewater 2[b]	0.0	16.8	—	1.61	17.9	−6.54
	15.5	30.4	94.1	1.25	—	—

[a] Average value of five measurements. [b] Wastewater 1 and wastewater 2 are the same wastewater sample. Wastewater 1 was analyzed by the sensor immediately after sampling and wastewater 2 was analyzed after two weeks storage at 4 °C.

4. Conclusions

In this work, the electrochemical behavior of Cyt c at Gra/Au NPs–Chit/GCE is investigated. The surface coverage of Cyt c shows that Gra/Au NPs–Chit nanocomposite provides a biocompatible microenvironment for the immobilization of Cyt c. DET between the Cyt c and Gra/Au NPs–Chit/GCE surface was obtained from the CV scan. The immobilized Cyt c on Gra/Au NPs–Chit film displays a quasi-reversible electrochemical behavior with a formal potential of −0.037 V (*vs.* SCE). The Cyt c–Gra/Au NPs–Chit/GCE possesses good electrocatalytic activity for the oxidation of NO_2^- at a low working potential. The graphene/gold nanoparticles-based redox protein sensor exhibits good sensitivity and stability for detecting NO_2^-. The fabrication of the proposed sensor is simple. It is easy to operate and exhibits a fast response time (5 s) to nitrite and has a long shelf-life (one month). The developed nitrite sensor is proven to be a reliable and accurate tool for the detection of nitrite in real samples. This study provides a new strategy for investigating the direct electrochemistry and application of the sensor.

Acknowledgements

Financial support from the National Natural Science Foundation of China (21075083 and 20927007) is gratefully acknowledged.

References

1 L. Wu, X. Zhang and H. Ju, *Anal. Chem.*, 2007, **79**, 453–458.
2 N. Karousis, T. Ichihashi, S. Chen, H. Shinohara, M. Yudasaka, S. Iijima and N. Tagmatarchis, *J. Mater. Chem.*, 2010, **20**, 2959–2964.
3 A. Düzgün, A. Maroto, T. Mairal, C. O'Sullivan and F. X. Rius, *Analyst*, 2010, **135**, 1037–1041.
4 A. K. Geim and K. S. Novoselov, *Nat. Mater.*, 2007, **6**, 183–191.
5 C. N. R. Rao, A. K. Sood, K. S. Subrahmanyam and A. Govindaraj, *Angew. Chem., Int. Ed.*, 2009, **48**, 7752–7777.
6 C. Shan, H. Yang, J. Song, D. Han, A. Ivaska and L. Niu, *Anal. Chem.*, 2009, **81**, 2378–2382.
7 Y. Zhou, S. Liu, H.-J. Jiang, H. Yang and H.-Y. Chen, *Electroanalysis*, 2010, **22**, 1323–1328.
8 B. Wang, J.-J. Zhang, Z.-Y. Pan, X.-Q. Tao and H.-S. Wang, *Biosens. Bioelectron.*, 2009, **24**, 1141–1145.
9 C. Guo, F. Hu, C. M. Li and P. K. Shen, *Biosens. Bioelectron.*, 2008, **24**, 819–824.
10 P. Yeh and T. Kuwana, *Chem. Lett.*, 1977, **6**, 1145–1148.
11 Q. Chen, S. Ai, X. Zhu, H. Yin, Q. Ma and Y. Qiu, *Biosens. Bioelectron.*, 2009, **24**, 2991–2996.
12 L. Zhang, *Biosens. Bioelectron.*, 2008, **23**, 1610–1615.
13 X. J. Chen, A. C. West, D. M. Cropek and S. Banta, *Anal. Chem.*, 2008, **80**, 9622–9629.
14 M. Liu, Y. Qi and G. Zhao, *Electroanalysis*, 2008, **20**, 900–906.
15 H.-H. Liu, J.-L. Lu, M. Zhang, D.-W. Pang and H. D. Abruña, *J. Electroanal. Chem.*, 2003, **544**, 93–100.
16 Y. Zhou, J. Zhi, Y. Zou, W. Zhang and S.-T. Lee, *Anal. Chem.*, 2008, **80**, 4141–4146.
17 S.-M. Chen and S.-V. Chen, *Electrochim. Acta*, 2003, **48**, 513–529.
18 J.-F. Wu, M.-Q. Xu and G.-C. Zhao, *Electrochem. Commun.*, 2010, **12**, 175–177.
19 R. Geng, G. Zhao, M. Liu and M. Li, *Biomaterials*, 2008, **29**, 2794–2801.
20 W. J. R. Santos, P. R. Lima, A. A. Tanaka, S. M. C. N. Tanaka and L. T. Kubota, *Food Chem.*, 2009, **113**, 1206–1211.
21 C. Xia, W. Ning and G. Lin, *Sens. Actuators, B-Chem.*, 2009, **137**, 710–714.
22 L. Cui, J. Zhu, X. Meng, H. Yin, X. Pan and S. Ai, *Sens. Actuators, B-Chem.*, 2012, **161**, 641–647.
23 J. Wang, P. Diao and Q. Zhang, *Analyst*, 2012, **137**, 145–152.
24 W. Hummers and R. Offeman, *J. Am. Chem. Soc.*, 1958, **80**, 1339.
25 N. I. Kovtyukhova, P. J. Ollivier, B. R. Martin, T. E. Mallouk, S. A. Chizhik, E. V. Buzaneva and A. D. Gorchinskiy, *Chem. Mater.*, 1999, **11**, 771–778.
26 G. Alarcón-Angeles, B. Pérez-López, M. Palomar-Pardave, M. T. Ramírez-Silva and A. M. S. Alegret, *Carbon*, 2008, **46**, 898–906.
27 T. Yin, W. Wei and J. Zeng, *Anal. Bioanal. Chem.*, 2006, **386**, 2087–2094.
28 L. Zhang, X. Jiang, E. Wang and S. Dong, *Biosens. Bioelectron.*, 2005, **21**, 337–345.
29 C. Liu, K. Wang, S. Luo, Y. Tang and L. Chen, *small*, 2011, **7**, 1203–1206.
30 Y. Chen, X.-J. Yang, L.-R. Guo, B. Jin, X.-H. Xia and L.-M. Zheng, *Talanta*, 2009, **78**, 248–252.
31 E. Laviron, *J. Electroanal. Chem.*, 1979, **100**, 263–270.
32 *Standard Methods for the Examination of Water and Wastewater*, ed. M. J. Taras, A. E. Greenberg, R. D. Hoak and M. C. Rand, American Public Health Association, Washington, D.C., 13th edn, 1971, pp. 240–243.

